Role of interface roughness scattering in self-consistent resonant-tunneling-diode simulations

Gerhard Klimeck,* Roger Lake, and Daniel K. Blanks
Raytheon Systems, 13532 N. Central Expressway MS35, Dallas, Texas 75243
(Received 22 January 1998)

The effects of interface roughness scattering in a resonant-tunneling diode are examined with the self-consistent Born and the multiple sequential scattering algorithm for various interface roughness correlation lengths. The effect of a self-consistent treatment of the scattering self-energies with the quantum charge and the electrostatic and exchange-correlation potentials is demonstrated. The effects of the scattering assisted charge and the exchange and correlation potential on the spurious bistability obtained in simulations of a symmetric resonant-tunneling diode is shown. [S0163-1829(98)05932-3]

I. INTRODUCTION

Resonant-tunneling diodes (RTD's) are now being developed[1] for circuit applications such as low power memory cells,[2] high speed adders,[3] high speed logic,[4] and analog-to-digital conversion.[5] RTD device design requirements vary dramatically with the specific application. For example, the required current densities can vary over four orders of magnitude.[2,3] Other design specifications are the voltage position of the main peak, the valley current density and the voltage of the second current turn-on. Quantitative modeling of such devices has already reduced the device development cycle time.

The electron transport through RTD's is governed by the electron charging, band structure, and scattering. Which one or combination of these effects principally govern the electron transport depends on the choice of material system, the device design, and the temperature of operation. To address the issues of quantitative device modeling in layered heterostructures we have developed a comprehensive device simulator[6–10] that addresses the modeling needs of device engineers and physicists. The theory underlying the nanoelectronic modeling (NEMO) tool is described in detail in Ref. 10.

Incoherent scattering is believed to be the source of the valley current in high-performance RTD's that have a large separation of the ground-state resonance and the higher excited states. Depending on the material system and device, interface roughness can be a strong scattering mechanism influencing the valley current of resonant tunneling diodes.[11–16] The purpose of this paper is to study the validity of common approximations used for modeling incoherent elastic scattering due to interface roughness. We compare RTD simulations with interface roughness scattering of various correlation lengths in the self-consistent Born (SCB) approximation and the multiple sequential scattering (MSS) approximation with and without scattering assisted charge self-consistency. Extensive citations for the various approaches for including incoherent scattering can be found in Refs. 11, 14, and 17.

The SCB treatment implies an infinite number of single, uncorrelated scattering events, which can imply a large number of iterations described in Ref. 10. Furthermore, if a self-consistent solution of the self-energies and Green functions is not achieved, current is not conserved. A finite-order approach that can be viewed as a truncation of the SCB algorithm[10] leads to a multiple sequential scattering algorithm similar to that described by Roblin and Liou.[11] This algorithm allows for an *a priori* number of scattering events and therefore limits the required CPU time.

Quantum charge self-consistent simulations typically predict bistable current-voltage characteristics for devices in which such an effect is not observed experimentally.[7,18] Despite intense theoretical investigation of intrinsic bistability since it was first experimentally observed,[19–22] the effect of the scattering assisted charge on the charge-self-consistency loop was only recently included.[7] In that work we presented a calculation in which a finite-order treatment of interface-roughness and polar-optical phonon scattering was iterated to convergence with a self-consistent treatment of the quantum charge.[7] Here we present a study of intrinsic bistability using a self-consistent Born treatment of interface-roughness scattering iterated to convergence with a self-consistent treatment of the quantum charge. This scattering assisted charge reduces the intrinsic bistability.

The incoherent scattering contributes to the current and the electron density that in turn, affects the electrostatic (Hartree) and exchange-correlation (XC) potentials. For interface roughness with larger correlation lengths, we show in Sec. III that a self-consistent treatment of the incoherent scattering with the quantum charge is essential to obtain physical results. In Sec. VI, we examine the effects of incoherent scattering assisted charge on the intrinsic bistability.

II. BASELINE NO-SCATTERING SIMULATION

The device we simulate in this paper is a nominally symmetric GaAs/AlAs RTD consisting of 3.1-nm barriers and a 6.2-nm well.[7,15,23,24] The RTD is clad with a 20-nm undoped spacer and high doping (1×10^{18} cm^{-3}) contact layers. We assign[15,24] the first and the third heterostructure interface to have interface roughness (see small inset of Fig. 1). The no-scattering simulations contain the virtual crystal approximation (VCA) contribution to the Hamiltonian on these sites.[10] All simulations are performed at 4.2 K to avoid Γ-X-Γ tunneling in the AlAs barriers. Exchange correlation is included in the local density approximation.[25] Figure 1 shows the result of a single band, quantum charge self-

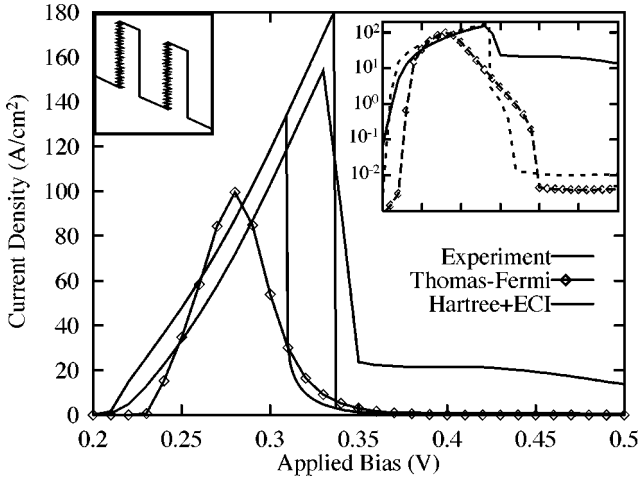

FIG. 1. Current voltage characteristics of a GaAs/AlAs RTD at 4.2 K. The Thomas-Fermi (semiclassical) potential solution generates an I-V characteristic that does not even fit the peak correctly. The no-scattering Hartree+XC self-consistent potential reproduces the RTD peak correctly, but it underestimates the valley current significantly (see larger inset, I-V on logarithmic scale). The experimental data shows a pronounced phonon peak in the valley current region. Small inset: conduction-band profile under positive bias indicating the rough interfaces.

consistent simulation without any scattering and a simulation based on a semiclassical Thomas-Fermi potential. The charge self-consistency includes the electrostatic potential as well as the XC potential. The I-V based on the semiclassical (Thomas-Fermi) potential does not fit the shape, the peak voltage, or the current values of the experimental data. Quantum charge self-consistency shifts the peak to higher voltages and spreads out the shape of the I-V peak to match the experimental data.[9] The valley current, however, is underestimated by three orders of magnitude (see larger inset of Fig. 1).

The quantum charge self-consistent simulation is performed in a forward and reverse bias sweep with the same polarity. A voltage region of bistability of 30 mV is evident in the simulation. This bistability emerges when either the potential or the charge of the previous bias point is used as an initial guess for the potential or charge of the next bias point. Note that the structure is nominally symmetric except for the interface roughness. We will discuss the bistability in more detail in Sec. VI.

The self-consistently calculated electrostatic potential and the XC potential can be stored and used as an input to a one-pass scattering calculation. We will refer to such a model as ''partial charge self-consistency.'' For the partial self-consistency calculations, we pick the potentials of the forward bias sweep. Both the dynamics and kinetics of the incoherent scattering affect the quantum charge. The incoherent scattering alters the position and width of the resonances which, in turn, affect the quantum charge. The incoherent scattering also opens up new channels for filling states that otherwise would not be filled. Both of these effects are ignored in the partial charge self-consistency model. We will refer to our model in which the quantum charge is calculated in the presence of incoherent scattering and iterated to convergence with the electrostatic and exchange-correlation po-

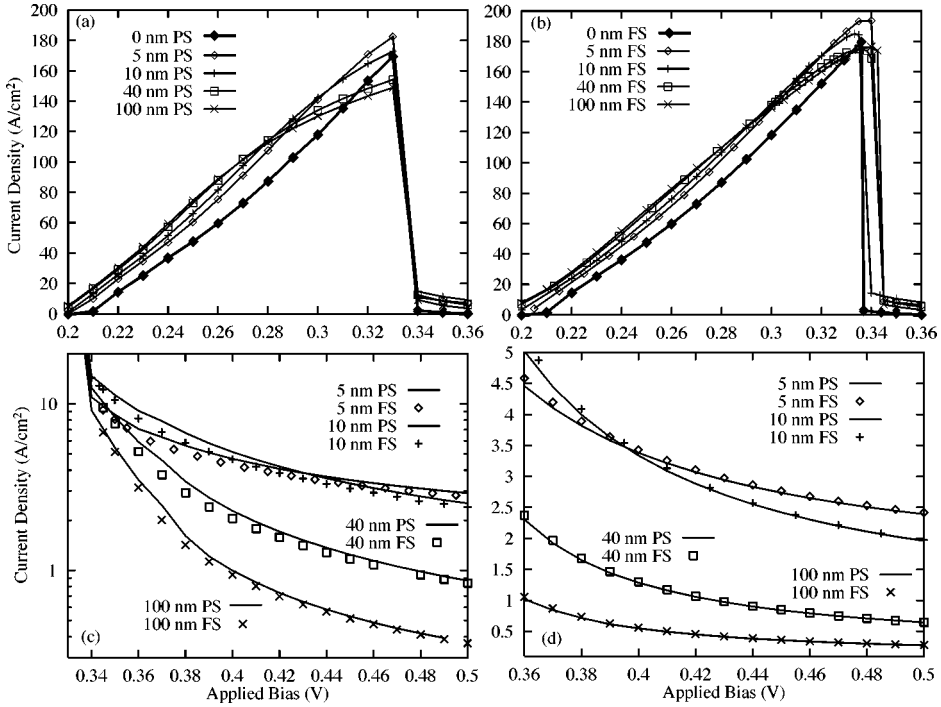

FIG. 2. Current-voltage characteristics calculated for five different interface roughness correlation lengths (Λ=0, 5, 10, 40, and 100 nm). The interface roughness is treated in the self-consistent Born approximation. (a) Partial self-consistency (PS). Scattering introduces a strong reduction of the peak current density and deforms the I-V peak shape. (b) Full charge self-consistency (FS). The peak amplitude does not change significantly anymore with the strength of the scattering and the shape of the I-V curve is maintained. (c) Valley current computed for PS and FS. The FS curves are shifted to slightly *lower* voltages due to the XC interaction. (d) Same as (c) without the XC potential. FS and PS now provide identical results in the valley current due to the low charge density.

tentials as ''full charge self-consistency.'' The nomenclature ''full'' is used as a convenient contrast to ''partial'' and does not imply the full solution of the many-particle Hamiltonian.

In this paper we are not intending to quantitatively simulate the valley current, but to examine the effects of the scattering assisted charge in self-consistent RTD simulation using the multiple sequential scattering and the self-consistent Born algorithms. Refs. 7, 15, and 23 show that the valley current can be properly modeled with the inclusion of polar optical phonon and interface roughness scattering.

III. SELF-CONSISTENT BORN TREATMENT OF SCATTERING INCLUDING QUANTUM CHARGE SELF-CONSISTENCY

Scattering assisted electron flow contributes to the valley current of RTD's, which implies an alteration of the occupation of the well. Scattering also alters the resonance spectrum (e.g., a damped oscillator has generally speaking a lowered frequency) and therefore changes the occupancy at peak current. Previous work ignored the effects of the interface roughness scattering on the self-consistency with the electrostatic and the XC potential.[11,13–15,12] We examine this assumption here with four different interface roughness correlation lengths ($\Lambda=5$, 10, 40, 100 nm) using an exponential correlation model.[10,15] Note that the $\Lambda=0$ nm curves are coherent tunneling calculations with the VCA treatment of the interface layer.

Figure 2(a) shows the NEMO simulation based on partial self-consistency. As the correlation length is increased, the peak current amplitude is reduced and the peak itself is deformed. All four curves show an identical turn-off, which is determined by the turn-off of the no-scattering potential calculation.

Figure 2(b) is based on full charge self-consistent potentials. The peak amplitude varies less strongly with the correlation length and a qualitatively correct shape of the I-V peak is maintained. The peak turn-on can be shifted by the scattering interaction. Comparing Figs. 2(a) and 2(b) we see that partial self-consistency provides reasonable results for the smaller correlation lengths.

Figure 2(c) compares the partial and the full charge self-consistent results of Figs. 2(a) and 2(b) in the valley current region. The current in the valley current region is one order of magnitude smaller than the peak current density. Therefore the electron density inside the well is about one order of magnitude smaller than at peak current flow. Since the charge density is relatively low we would therefore expect no difference in the partial and the full charge self-consistency. However, surprisingly we find a small difference between the two approaches. The full self-consistency results are shifted slightly to smaller voltages. This is contrary to to the expectation that charge-self-consistency shifts the I-V curve to higher voltages (see Fig. 1). In Fig. 2(d) we show that this shift to smaller voltages is due to the XC potential. We show in that figure the partial and the full self-consistency results *without* the XC potential and we find identical results as expected from our low charge-density reasoning.

IV. COMPARISON OF SELF-CONSISTENT BORN AND MULTIPLE SEQUENTIAL SCATTERING WITH PARTIAL SELF-CONSISTENCY

For elastic scattering, the self-consistent Born approximation requires a self-consistent solution of G^R with Σ^R and

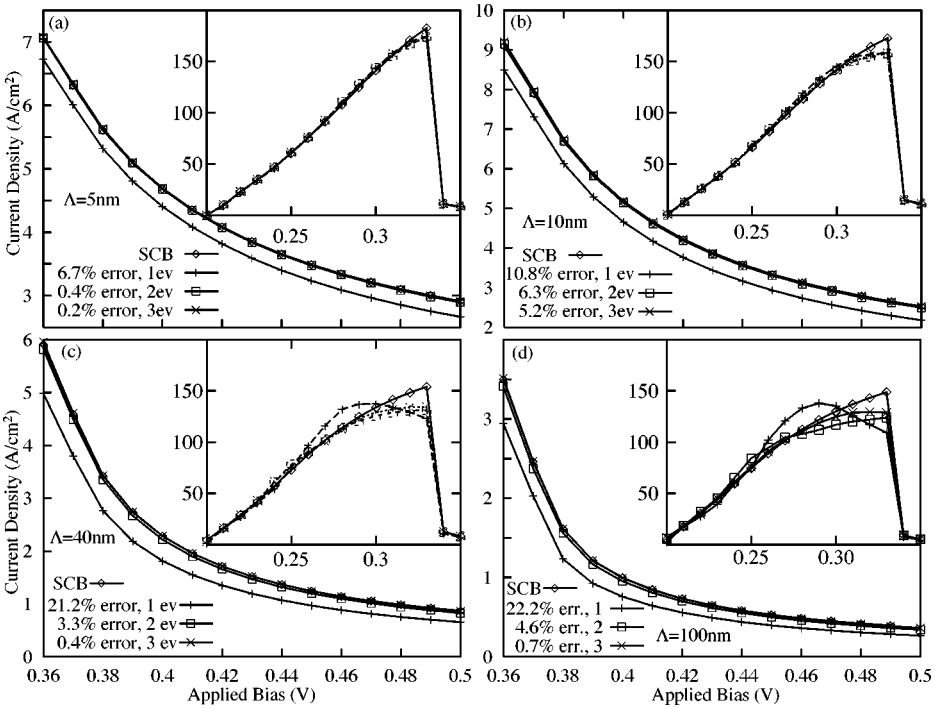

FIG. 3. Valley current and peak current (insets) densities for four different interface roughness correlation lengths ($\Lambda=5$, 10, 40, and 100 nm) calculated in the MSS algorithm for 1, 2, and 3 scattering events compared against the SCB result. The increasing correlation length corresponds to an increasing scattering strength and it shows stronger deviations. For large interaction strengths the peak current density is significantly distorted in the case of few scattering events.

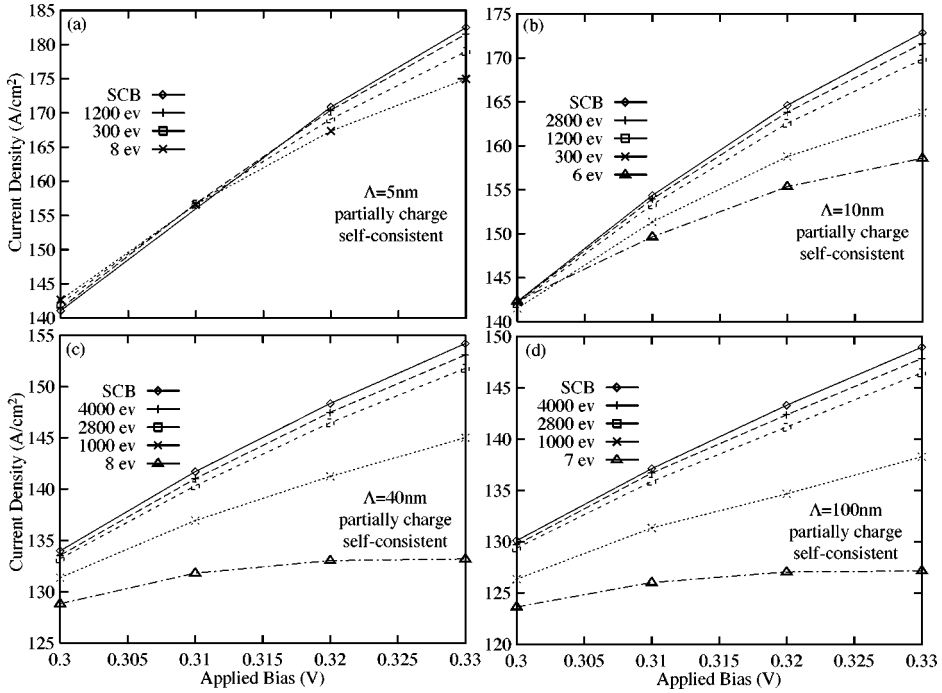

FIG. 4. Peak current density calculated with partial charge self-consistency for four different interface roughness correlation lengths (Λ=5, 10, 40, and 100 nm) calculated in the MSS algorithm compared against the SCB result. The stronger the interaction strength the more scattering events are needed in the MSS algorithm to converge to the SCB result.

$G^<$ with $\Sigma^<$ (for details see Ref. 10). The self-consistent solution of G^R with Σ^R generates a continued fraction expansion which converges fast with typical numbers of convergence of 7–25. The self-consistent solution of $G^<$ with $\Sigma^<$ generates a power series expansion that converges slowly with typical numbers ranging from 25 to 10,000.

For reasons of numerical tractability, we developed a finite-order approach based on a truncation of the self-consistent Born expansions.[10] This algorithm sets an *a priori* number of scattering events that are included in the transport calculation. The truncation leads to a Green-function version of the multiple sequential scattering algorithm similar to that described in Ref. 11. Reference 10 details this algorithm and compares the two algorithms for two different structures and the same interface roughness correlation length. In this section we compare the two algorithms for the same structure with different interface roughness correlation lengths.

Figure 3 compares the valley current for four different interface roughness correlation lengths computed in the MSS algorithm for different numbers of scattering events (1–3) against the SCB baseline. The current is calculated with the partially self-consistent potential. With only one scattering event the valley current in the MSS algorithm deviates significantly from the SCB result. The deviation increases with the strength of the interaction which is proportional to the interface roughness correlation length (7–22 %). Two scattering events reduce the difference between the MSS and the SCB algorithm, leading to 0.4–4.6% deviation for the smaller correlation lengths of 5 nm and 10 nm. Three scattering events result in 0.2–0.7 % deviation for all correlation lengths. The current calculated in a second-order multiple sequential scattering approximation is essentially identical to the current calculated in a self-consistent Born approximation. The first-order calculation is very good. This is consistent with the ''capture'' point of view of Chevoir and Vinter[14] and the numerical result of Johansson.[26]

The insets in Fig. 3 compare the MSS algorithm for the same number of events (1–3) against the SCB algorithm at the main *I-V* peak. While the MSS algorithm delivers a qualitatively correct current for small interface roughness correlation lengths (5 nm and 10 nm), larger correlation lengths result in a significant distortion. Reference 10 already indicated that a large number of events may be necessary in the MSS algorithm to reproduce the SCB result. We show this effect for different correlation lengths in Fig. 4. The larger the correlation length the more scattering events are necessary to reproduce the SCB result. For Λ=5 nm, 1200 events in the MSS algorithm produce good agreement with the SCB calculation. For Λ=40 and Λ=100 nm, 4000 events are needed.

V. COMPARISON OF SELF-CONSISTENT BORN AND MULTIPLE SEQUENTIAL SCATTERING WITH FULL SELF-CONSISTENCY

Section IV compared the MSS and the SCB algorithm based on partial self-consistency. The scattering was shown to be strong enough to distort the main peak of the MSS based current if only a few scattering events were considered. Since the current density is proportional to the charge density inside the device we expect the charge density to be strongly modified for the limited number of scattering events as well.

Figure 5 compares the SCB and MSS algorithms for fully charge self-consistent calculations. The MSS algorithm is evaluated with a different number of events for the four different correlation lengths against the SCB algorithm. For the shorter correlation lengths of 5 and 10 nm, Figs. 5(a) and

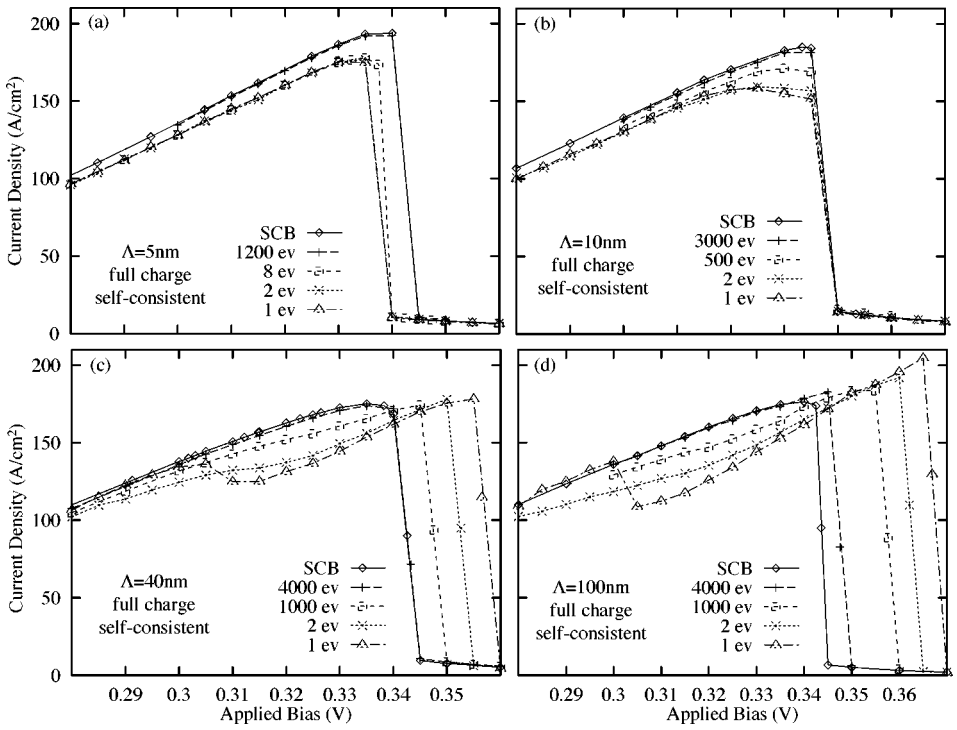

FIG. 5. Peak current density computed in full charge self-consistency in the MSS compared to the SCB algorithm for four different interface roughness correlation lengths ($\Lambda = 5$, 10, 40, and 100 nm). Strong interactions computed with too few scattering events cause spurious modulations on the peak. These modulations cannot be attributed to the existence of two parallel RTD's but to the limits of the MSS algorithm. If enough scattering events are added to the computation, the SCB result, which does not show and double peak, is approached.

5(b) show a qualitatively correct shape of the MSS *I-V* curves for even one scattering event. For the longer correlation lengths of 40 and 100 nm, Figs. 5(c) and 5(d) initially show a spurious double-peak feature. However, this double-peak feature vanishes as the number of scattering events is increased.

It was, at first, tempting to interpret the double-peak feature in the *I-V* as numerical evidence of two parallel RTD's with different well and barrier lengths. Such an argument is supported by a split resonance spectral function as shown in Fig. 6. However, as the number of scattering events is increased, the spectral function reverts to a single, broadened peak. The splitting of the resonance does not appear, when the real part of the scattering self-energies is neglected.[24]

VI. INCOHERENT SCATTERING AND INTRINSIC BISTABILITY

Charge-self-consistent simulations of RTD's often either predict intrinsic bistability for nominally symmetric structures in which such an effect is not observed experimentally,[18,7] or they predict a too large bistable voltage region. Zou *et al.*[18] pointed out that they were able to eliminate the bistability when the XC potential was included in the simulation. We have implemented the XC potential using the local-density approximation (LDA) and found that, in general, the bistability does persist even with this interaction.[7] Figure 7(b) compares two simulations without and with the exchange and correlation potential *without* scattering. Clearly the bistability is reduced with the inclusion of the exchange and correlation interaction, however a bistability region of about 30 mV still exists.

Scattering increases the well charge density in the valley current region. This increase in the charge density changes the electrostatic and the XC potential. Figure 7(a) shows that scattering alone *without* the inclusion of the XC reduces the bistability region significantly for two different interface roughness correlation lengths. The actual reduction of the bistability region is dependent on the correlation length. Figure 7(a) shows that the bistability region is smaller for the correlation length with the larger valley current. In Fig. 7(b) we show the sequence of curves in which we reduce the bistability region starting from the no-scattering, no XC case with the inclusion of XC, and then the inclusion of scattering. A bistability region still persists, however. We will examine this bistability in more detail in a future publication as a function of scattering mechanisms and scattering strengths.

VII. SUMMARY

We have presented the first comparison of the MSS and SCB algorithms for including interface roughness scattering in which the scattering-assisted quantum charge is iterated to convergence with the Hartree and exchange-correlation potentials. The MSS algorithm is found to provide good estimates for the valley current with only a few scattering events. However, the advantages of the MSS over the SCB algorithm disappear for the peak current when the scattering is strong and the natural linewidth is narrow. In such circumstances, using an insufficient number of scattering events, the MSS algorithm can give rise to spurious features in the peak current which mimic the effect of two parallel RTD's with different well widths. The MSS algorithm does converge towards the SCB result and any spurious features disappear if a

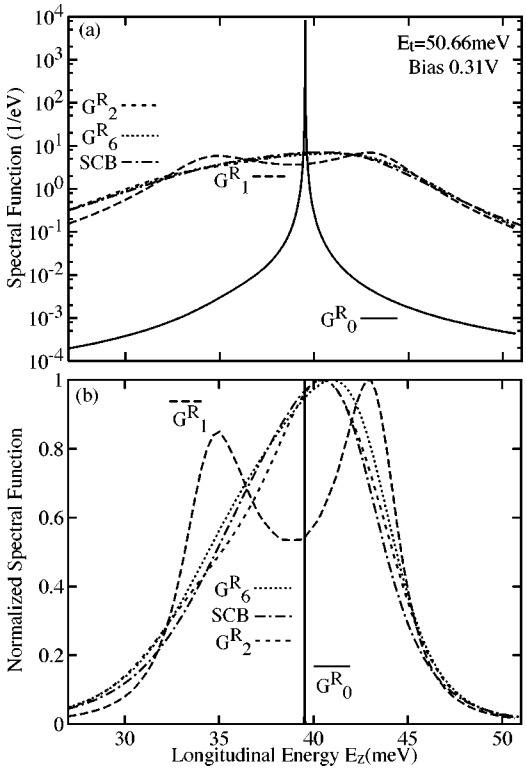

FIG. 6. Spectral functions $[-(1/\pi)\mathrm{Im}\{G_i^R\}]$ on a logarithmic (a) and normalized linear (b) scale for various scattering orders as a function of longitudinal energy E_z. The total energy is 50.66 meV and the bias 0.31 V. The logarithmic scale shows clearly how sharp the natural linewidth is compared to the scattering broadened linewidth. The linear scale shows the split first-order spectral function. Higher orders do not show this split behavior and smooth out with increasing number of scattering events and converge towards the SCB result.

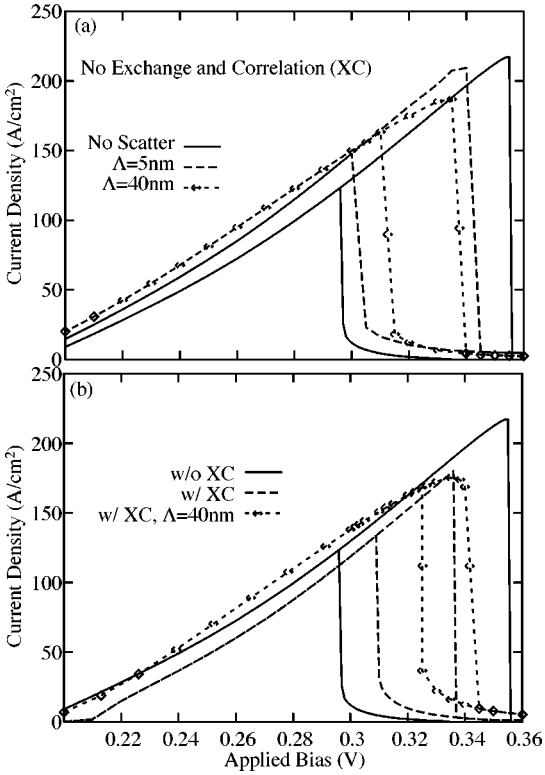

FIG. 7. Effect of scattering and XC potential on the bistability at the RTD turn-off. (a) Effect of scattering alone without the XC potential. Scattering reduces the bistability region. The higher the valley current, the smaller the bistability region. (b) Effect of XC and scattering combined. Both XC and scattering reduce the bistability; however, a small bistability region remains.

sufficient number of scattering events is included. Finally, bistability is reduced but not removed by including the incoherently scattering assisted charge and/or the exchange and correlation interaction in the potential calculations.

ACKNOWLEDGMENTS

We would like to thank R. Chris Bowen, Chenjing L. Fernando, Manhua Leng, and William R. Frensley for their work during the NEMO software project. We would like to thank Ted Moise and Yung-Chung Kao for the experimental data during the NEMO project.

*Present address: Jet Propulsion Laboratory, 4800 Oak Grove Dr., MS 168-522, Pasadena, CA 91109-8099. Electronic address: gekco@jpl.nasa.gov

[1] A. Seabaugh, B. Brar, T. P. E. Broekaert, G. Frazier, F. Morris, P. van der Wagt, and E. Beam III, in the *19th Annual GaAs IC Symposium Technical Digest* (IEEE, Piscataway, NJ, 1997), pp. 119–122.

[2] J. P. A. van der Wagt, A. C. Seabaugh, and E. Beam III, Electron Device Lett. **19**, 7 (1998).

[3] L. J. Micheel, A. H. Taddiken, and A. C. Seabaugh, in *The Proceedings of the Twenty-Third International Symposium on Multi-Valued Logic* (IEEE, Piscataway, NJ, 1993), p. 164.

[4] W. Williamson, III, S. B. Enquist, D. H. Chow, H. L. Dunlap, S. Subramanian, P. Lei, G. H. Bernstein, and B. K. Gilbert, IEEE J. Solid-State Circuits **32**, 222 (1997).

[5] T. P. E. Broekaert, B. Brar, J. P. A. van der Wagt, A. C. Seabaugh, T. S. Moise, F. S. Morris, E. Beam III, and G. A. Frazier (unpublished).

[6] G. Klimeck, R. Lake, R. C. Bowen, W. R. Frensley, and D. Blanks, in the *1995 53rd Annual Device Research Conference Digest* (IEEE, NJ, 1995), p. 52.

[7] R. Lake, G. Klimeck, R. C. Bowen, C. Fernando, D. Jovanovic, D. Blanks, T. S. Moise, Y. C. Kao, M. Leng, and W. R. Frensley, in *The 1996 54th Annual Device Research Conference Digest* (IEEE, NJ, 1996), p. 174.

[8] G. Klimeck, T. Boykin, R. C. Bowen, R. Lake, D. Blanks, T. S. Moise, Y. C. Kao, and W. R. Frensley, in *The 1997 55th Annual Device Research Conference Digest* (IEEE, NJ, 1997), p. 92.

[9] G. Klimeck, R. Lake, R. C. Bowen, W. R. Frensley, and T. S. Moise, Appl. Phys. Lett. **67**, 2539 (1995).

[10] r. Lake, G. Klimeck, R. C. Bowen, and D. Jovanovic, J. Appl. Phys. **81**, 7845 (1997).

[11] P. Roblin and W. R. Liou, Phys. Rev. B **47**, 2146 (1993).

[12] P. Roblin, R. C. Potter, and A. Fathimulla, J. Appl. Phys. **79**, 2502 (1996).

[13] S.-J. Wang, J.-C. Lin, W.-R. Liou, M. ling Yeh, Y.-C. Luo, and C.-Y. Cheng, Jpn. J. Appl. Phys., Part 1 **35**, 3858 (1996).

[14] F. Chevoir and B. Vinter, Phys. Rev. B **47**, 7260 (1993).

[15] R. Lake, G. Klimeck, R. C. Bowen, C. Fernando, M. Leng, T. Moise, and Y. C. Kao, Superlattices Microstruct. **20**, 279 (1996).
[16] R. Lake, G. Klimeck, and D. K. Blanks, Semicond. Sci. Technol. **13**, A163 (1998).
[17] M. V. Fischetti, J. Appl. Phys. **83**, 270 (1998).
[18] N. Zou, M. Willander, I. Linnerud, U. Hanke, K. A. Chao, and Y. M. Galperin, Phys. Rev. B **49**, 2193 (1994).
[19] V. J. Goldman, D. C. Tsui, and J. E. Cunningham, Phys. Rev. Lett. **58**, 1256 (1987).
[20] T. C. Sollner, Phys. Rev. Lett. **59**, 1622 (1987).
[21] A. Zaslavsky, J. V. Goldman, D. C. Tsui, and J. E. Cunningham, Appl. Phys. Lett. **53**, 1408 (1988).
[22] E. S. Alves, L. Eaves, M. Henini, O. H. Hughes, M. L. Leadbeater, F. W. Sheard, G. A. Toombs, G. Hill, and M. A. Pate, Electron. Lett. **24**, 1190 (1988).
[23] G. Klimeck, R. Lake, C. L. Fernando, R. C. Bowen, D. Blanks, M. Leng, T. Moise, Y. C. Kao, and W. R. Frensley, in *Quantum Devices and Circuits*, edited by K. Ismail, S. Bandyopadhyay, and J. P. Leburton (Imperial College Press, London, 1997), pp. 154–159.
[24] G. Klimeck, R. Lake, and D. K. Blanks, Semicond. Sci. Technol. (to be published).
[25] E. Gawlinski, T. Dzurak, and R. A. Tahir-Kheli, J. Appl. Phys. **72**, 3562 (1992).
[26] P. Johansson, Phys. Rev. B **48**, 8938 (1993).